Adapting Reference Vectors and Scalarizing Functions by Growing Neural Gas to Handle Irregular Pareto Fronts *Supplementary Material*

Yiping Liu, *Member, IEEE*, Hisao Ishibuchi, *Fellow, IEEE*, Naoki Masuyama, *Member, IEEE*, and Yusuke Nojima, *Member, IEEE*

***Abstract*—This is the supplementary material for Adapting Reference Vectors and Scalarizing Functions by Growing Neural Gas to Handle Irregular Pareto Fronts. This supplementary material provides (1) the further comparisons among DEA-GNG and nine other algorithms, (2) the complexity analysis of DEA-GNG, and (3) the further investigations on the behavior of DEA-GNG.**

I. Further Comparisons among Different Algorithms

A. Comparison Using Hypervolume

In Table I, we show the results of hypervolume (HV) [1] and the performance scores obtained by DEA-GNG, DEA-GNG*, A-NSGA-III [2], RVEA* [3], AdaW [4], MOEA/D-LTD [5], MOEA/D-AWA [6], MOEA/D-SOM [7], MOEA/D-PaS [8], and MOEA/D [9] on 34 test problems listed in Table I in the main body of the paper. The average HV value and the corresponding performance score [1] of each algorithm on each test problem are given in Table I. A darker tone corresponds to a larger performance score. For each test problem, the performance score of an algorithm is the number of the comparative algorithms which perform significantly worse than it according to HV. Moreover, we give the average performance score of each algorithms over all the test problems at the bottom of Table I. Note that when calculating HV in this study, a solution set obtained by an algorithm is normalized based on the true Pareto front, and the reference point is set to $(1.1, \ldots, 1.1)$.

This work was supported by National Natural Science Foundation of China (Grant No. 61876075 and 61803192), the Program for Guangdong Introducing Innovative and Enterpreneurial Teams (Grant No. 2017ZT07X386), Shenzhen Peacock Plan (Grant No. KQTD2016112514355531), the Science and Technology Innovation Committee Foundation of Shenzhen (Grant No. ZDSYS201703031748284), the Program for University Key Laboratory of Guangdong Province (Grant No. 2017KSYS008), and JSPS KAKENHI (Grant No. 19K20358).

Y. Liu, N. Masuyama, Y. Nojima are with Department of Computer Science and Intelligent Systems, Graduate School of Engineering, Osaka Prefecture University, Sakai, Osaka 599-8531, Japan. (yiping0liu@gmail.com, masuyama@cs.osakafu-u.ac.jp, nojima@cs.osakafu-u.ac.jp)

H. Ishibuchi is with Shenzhen Key Laboratory of Computational Intelligence, University Key Laboratory of Evolving Intelligent Systems of Guangdong Province, Department of Computer Science and Engineering, Southern University of Science and Technology, Shenzhen 518055, China. (hisao@sustech.edu.cn) (*Corresponding Author*)

We can see from Table I that DEA-GNG generally performs best according to the average performance score, followed by the other algorithms. This general observation is similar to that from the results of IGD^+ in the main body of the paper. One can notice that there are some inconsistencies between the results of HV and IGD^+ on some test problems. That is, an algorithm may have a small (or large) performance score on a test problem according to HV or IGD^+ but have a large (or small) one according to the other indicator. One reason is that the evaluation by HV depends on the setting of the reference point when the PF shape is irregular [10]. Another reason is that HV and IGD^+ have different preferences on evaluation. Although both HV and IGD^+ measure the convergence and diversity performance of a solution set simultaneously, IGD^+ evaluates the performance of a solution set based on the true Pareto front, while HV does not. The IGD^+ value is calculated by the distance between the reference points on the true Pareto front and the solutions set. A solution set with a larger HV does not necessarily closer to the reference points, and vice versa. This phenomenon implies that the obtained solution sets are not comparable in terms of the dominance relation of sets. In other words, different decision makers may have different preference to them, which is quite natural. Please refer to [11] for a detailed discussion.

B. Visualized Comparison

In this subsection, we visualize the final solution sets obtained by different algorithms in a single run on Scaled DTLZ2-3 and DTLZ7-8 as well as the true PFs in Figs. 1 and 2, respectively. This particular run is associated with the result which is the closest to the mean IGD^+ value in Table II in the main body of the paper. Note that the objective values of the solutions have been normalized based on the true PF. The reason of choosing these test problems is that we would like to observe the behavior of different algorithms in handling a relatively simple PF (i.e., SDTLZ2-3's) and a complicated one (i.e., DTLZ7-8's), respectively.

From Fig. 1 we can see that the solution sets obtained by DEA-GNG, DEA-GNG*, AdaW, and MOEA/D-LTD are well distributed according to the PF shape. MOEA/D has a normalization issue. For the others, the adaptation strategy more or less affects the uniformity of solutions.

TABLE I
RESULTS OF HV.

HV	DEA-GNG	DEA-GNG*	A-NSGA-III	RVEA*	AdaW	MOEA/D-LTD	MOEA/D-AWA	MOEA/D-SOM	MOEA/D-PaS	MOEA/D
Scaled DTLZ2-2	4.204E-1 9	4.203E-1 8	4.178E-1 1	4.201E-1 7	4.200E-1 5	4.193E-1 2	4.200E-1 5	4.070E-1 0	4.194E-1 3	4.195E-1 4
Scaled DTLZ2-3	7.428E-1 5	7.426E-1 5	7.378E-1 2	7.401E-1 4	7.429E-1 5	7.452E-1 7	7.428E-1 5	6.511E-1 0	7.342E-1 1	7.373E-1 2
Scaled DTLZ2-5	1.140E+0 3	1.129E+0 2	1.275E+0 9	1.189E+0 6	1.261E+0 7	1.270E+0 8	1.159E+0 4	8.719E-1 1	1.151E+0 4	7.207E-1 0
Scaled DTLZ2-8	1.688E+0 4	1.686E+0 4	1.910E+0 9	1.501E+0 2	1.882E+0 7	1.884E+0 7	1.694E+0 4	1.510E+0 2	1.084E+0 1	6.964E-1 0
Convex DTLZ2-2	8.715E-1 8	8.713E-1 7	8.689E-1 1	8.707E-1 4	8.705E-1 4	8.698E-1 2	8.716E-1 8	8.632E-1 0	8.705E-1 4	8.702E-1 2
Convex DTLZ2-3	1.277E+0 2	1.278E+0 2	1.277E+0 2	1.278E+0 4	1.278E+0 5	1.277E+0 2	1.278E+0 5	1.275E+0 0	1.278E+0 6	1.275E+0 0
Convex DTLZ2-5	1.596E+0 2	1.596E+0 2	1.608E+0 6	1.609E+0 7	1.601E+0 4	1.606E+0 6	1.609E+0 8	1.556E+0 0	1.603E+0 5	1.589E+0 1
Convex DTLZ2-8	2.128E+0 2	2.126E+0 2	2.138E+0 5	2.140E+0 6	2.133E+0 2	2.139E+0 5	2.143E+0 9	2.143E+0 8	2.111E+0 1	2.073E+0 0
Minus-DTLZ2-2	9.912E-1 7	9.912E-1 7	9.866E-1 3	9.909E-1 6	9.863E-1 2	9.883E-1 4	9.911E-1 7	9.471E-1 0	9.894E-1 5	9.844E-1 1
Minus-DTLZ2-3	7.215E-1 6	7.210E-1 6	6.967E-1 2	7.218E-1 6	7.211E-1 6	6.895E-1 1	7.088E-1 4	6.605E-1 0	7.014E-1 3	7.082E-1 4
Minus-DTLZ2-5	1.959E-1 9	1.700E-1 6	1.134E-1 4	1.803E-1 8	1.699E-1 6	7.411E-2 1	1.010E-1 3	3.669E-2 0	7.314E-2 1	1.581E-1 5
Minus-DTLZ2-8	9.887E-3 9	7.831E-3 6	3.612E-3 1	8.392E-3 8	3.775E-3 1	4.530E-3 3	2.691E-3 0	7.822E-3 6	5.395E-3 4	6.049E-3 5
DTLZ2BZ-2	5.712E-1 7	5.706E-1 5	5.684E-1 1	5.713E-1 8	5.683E-1 1	5.703E-1 4	5.714E-1 9	5.571E-1 0	5.705E-1 4	5.690E-1 3
DTLZ2BZ-3	7.026E-1 6	7.014E-1 6	6.964E-1 3	7.001E-1 5	7.048E-1 7	6.942E-1 3	7.037E-1 6	5.993E-1 0	6.698E-1 1	6.854E-1 2
DTLZ2BZ-5	8.106E-1 8	7.831E-1 6	7.507E-1 4	7.961E-1 6	1.095E+0 9	6.863E-1 3	6.182E-1 2	4.698E-1 1	3.346E-1 0	7.720E-1 5
DTLZ2BZ-8	1.391E+0 6	1.301E+0 4	1.495E+0 8	1.308E+0 4	1.502E+0 8	1.091E+0 2	1.256E+0 3	7.378E-1 1	3.901E-1 0	1.452E+0 7
DTLZ5-3	2.664E-1 8	2.665E-1 9	2.622E-1 4	2.656E-1 7	2.654E-1 6	2.562E-1 2	2.624E-1 4	2.540E-1 1	2.557E-1 1	2.457E-1 0
DTLZ5-5	1.136E-1 1	2.296E-2 0	7.269E-2 0	1.782E-1 7	1.227E-1 2	1.467E-1 4	1.536E-1 6	2.010E-1 8	1.467E-1 4	2.031E-1 8
DTLZ5-8	7.722E-2 2	3.908E-5 0	5.805E-3 0	2.015E-1 5	6.836E-2 2	2.077E-1 6	2.142E-1 8	2.078E-1 7	7.964E-2 2	2.233E-1 8
DTLZ7-2	5.444E-1 6	5.444E-1 6	5.444E-1 6	5.349E-1 4	5.416E-1 5	5.239E-1 3	5.442E-1 6	2.008E-1 0	4.321E-1 1	4.624E-1 2
DTLZ7-3	5.636E-1 7	5.612E-1 6	5.538E-1 4	5.648E-1 8	5.673E-1 9	5.572E-1 5	5.456E-1 3	4.168E-1 0	4.220E-1 1	5.196E-1 2
DTLZ7-5	5.335E-1 7	4.985E-1 5	4.547E-1 4	5.281E-1 7	5.288E-1 7	5.217E-1 6	2.681E-1 1	3.299E-1 2	3.501E-1 3	1.391E-1 0
DTLZ7-8	5.154E-1 9	4.259E-1 6	3.733E-1 2	3.507E-1 2	3.548E-1 2	5.011E-1 8	3.561E-1 2	1.108E-1 1	4.267E-1 6	5.726E-3 0
WFG1-2	7.970E-1 3	7.967E-1 2	8.193E-1 7	7.683E-1 1	8.067E-1 3	7.894E-1 2	8.355E-1 9	8.225E-1 8	5.899E-1 0	8.056E-1 3
WFG1-3	1.249E+0 4	1.250E+0 4	1.256E+0 9	1.250E+0 4	1.254E+0 8	1.242E+0 3	1.250E+0 4	1.143E+0 1	1.053E+0 0	1.209E+0 2
WFG1-5	1.598E+0 6	1.578E+0 3	1.603E+0 8	1.464E+0 0	1.599E+0 6	1.603E+0 8	1.581E+0 5	1.569E+0 2	1.589E+0 4	1.521E+0 1
WFG1-8	2.140E+0 6	2.126E+0 4	2.141E+0 6	1.811E+0 0	2.131E+0 5	2.139E+0 6	2.143E+0 6	2.036E+0 2	2.079E+0 3	1.764E+0 0
WFG2-2	7.651E-1 7	7.647E-1 6	7.647E-1 7	7.639E-1 5	7.611E-1 2	7.634E-1 4	7.650E-1 6	7.582E-1 1	7.624E-1 3	7.400E-1 0
WFG2-3	1.233E+0 5	1.233E+0 5	1.234E+0 5	1.230E+0 2	1.237E+0 9	1.227E+0 2	1.229E+0 2	1.206E+0 1	1.232E+0 5	1.194E+0 0
WFG2-5	1.561E+0 5	1.540E+0 3	1.584E+0 6	1.556E+0 4	1.587E+0 7	1.594E+0 9	1.580E+0 6	1.442E+0 0	1.445E+0 0	1.488E+0 2
WFG2-8	2.128E+0 5	2.127E+0 5	2.128E+0 5	2.057E+0 2	2.109E+0 4	2.130E+0 5	2.125E+0 5	2.074E+0 3	7.463E-1 0	1.951E+0 1
Polygon-based Problem-3	3.794E-1 6	3.800E-1 6	3.737E-1 4	3.795E-1 6	3.835E-1 9	3.585E-1 2	3.746E-1 4	3.446E-1 0	3.489E-1 1	3.602E-1 3
Polygon-based Problem-5	2.009E-1 8	1.999E-1 7	1.881E-1 5	1.630E-1 0	2.004E-1 7	1.609E-1 0	1.656E-1 3	1.701E-1 4	1.632E-1 2	1.892E-1 5
Polygon-based Problem-8	6.899E-2 9	6.869E-2 8	6.442E-2 6	4.458E-2 1	6.826E-2 7	5.308E-2 2	3.742E-2 0	6.233E-2 5	6.164E-2 4	5.553E-2 3
Average Performance Score	5.794	4.794	4.382	4.588	5.265	4.029	4.765	1.912	2.441	2.382

In Fig. 2, the solution sets are shown by parallel coordinates. Please refer to [12] for how to read many-objective solution sets in parallel coordinates. We can observe from Fig. 2 that DEA-GNG, DEA-GNG*, A-NSGA-II, RVEA*, and AdaW can maintain good diversity, while the others cannot. Moreover, DEA-GNG*, A-NSGA-II, RVEA*, and AdaW obtained a number of solutions whose objective values are larger than 1. These solutions are not very close to the true PF. Therefore, only DEA-GNG obtained a solution set with good diversity and convergence.

C. Friedman rank test for the Results of IGD$^+$ and HV

In this subsection, we use the Friedman rank test [13] to determine whether there is a significant difference among the comparative algorithms for the results of IGD$^+$ and HV. The null hypothesis is rejected at a significant level of 0.05.

Tables II and III show the Friedman rank test for the results of IGD$^+$ and HV, respectively. We can see from Tables II and III that our DEA-GNG has the highest ranking, and the p-values show that there is a significant difference among the algorithms for results of both IGD$^+$ and HV.

In addition, since the Friedman rank test only can detect significant differences over the whole multiple comparison, we use a post-hoc test to obtain a p-value which determines the degree of rejection of the hypothesis between each pair of algorithms. The p-value of every hypothesis is obtained through the conversion of the rankings computed by using a normal approximation. Tables IV and V show the pairwise hypotheses analyzed by the post-hoc test for the results of IGD$^+$ and HV, respectively. The p-values in Table IV show that the IGD$^+$ results obtained by DEA-GNG are significantly different from those of the other algorithms expect for DEA-GNG* and AdaW. The p-values in Table IV show that the HV results obtained by DEA-GNG are significantly different from the other algorithms expect for DEA-GNG*, AdaW, MOEA/D-AWA, and REVA*.

II. COMPLEXITY ANALYSIS

DEA-GNG includes two models: the DEA-based optimization model and the GNG-based learning model. Table VI lists the time complexity of each operator in these models and the total time complexity in one generation. Note that N is the population size.

In one generation, the time complexities of the operators in the DEA-based optimization model are the same to those in [14]. The total time complexity of this model is $O(N^2)$. Please refer to [14] for the details. In the GNG-based learning model, the time complexity of input signal archive update is

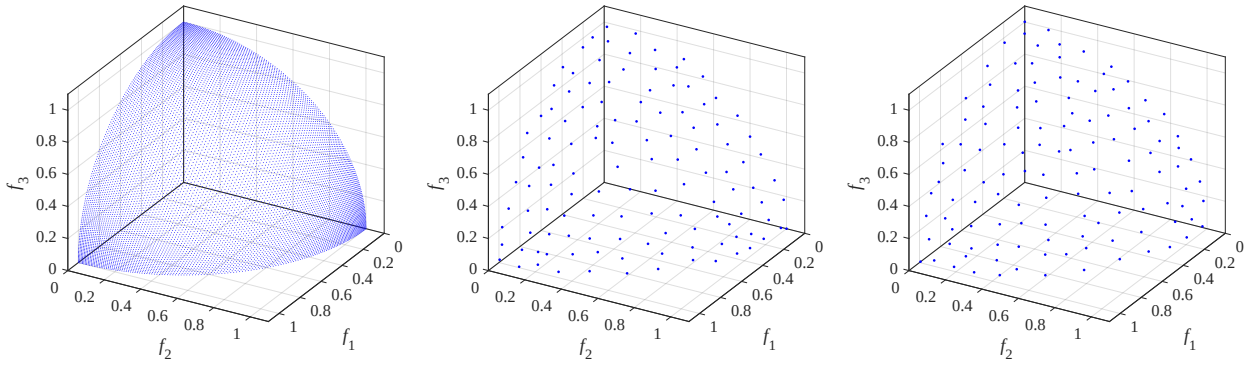

(a) True Pareto Front (b) DEA-GNG (c) DEA-GNG*

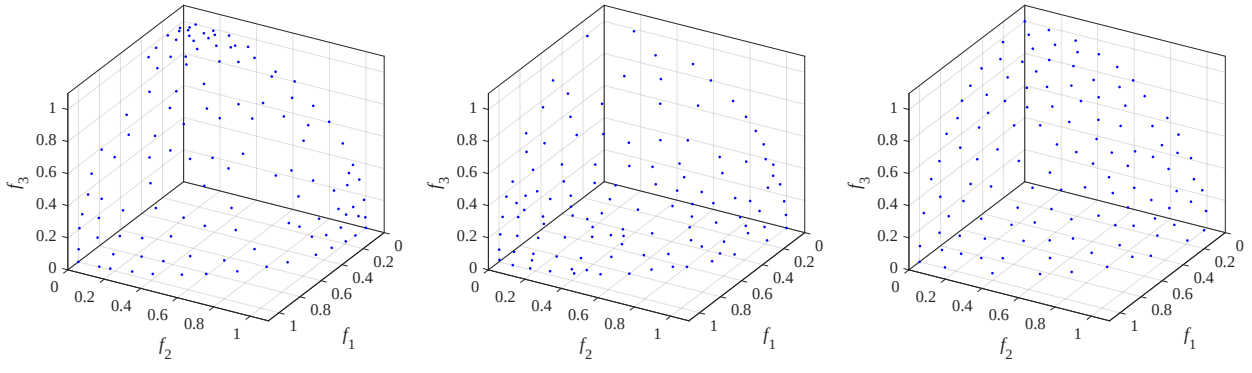

(d) A-NSGA-III (e) RVEA* (f) AdaW

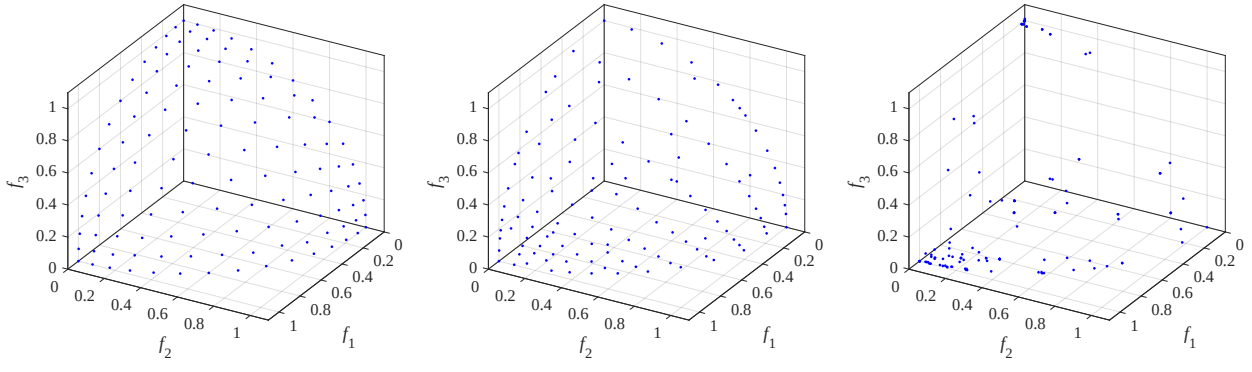

(g) MOEA/D-LTD (h) MOEA/D-AWA (i) MOEA/D-SOM

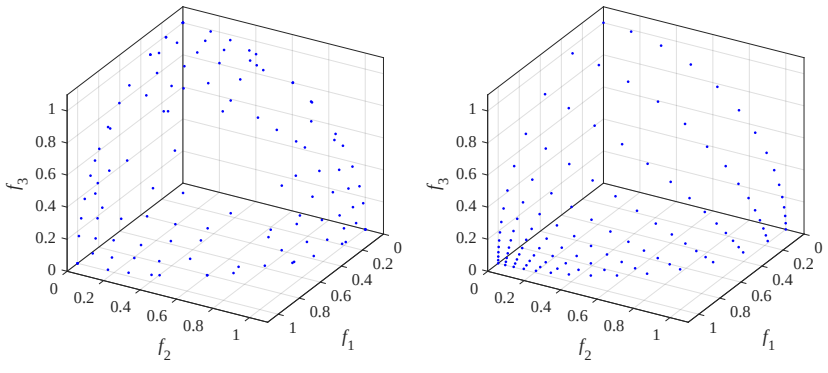

(j) MOEA/D-PaS (k) MOEA/D

Fig. 1. The true Pareto front and the the final solution sets obtained by different algorithm in a single run on Scaled DTLZ2-3.

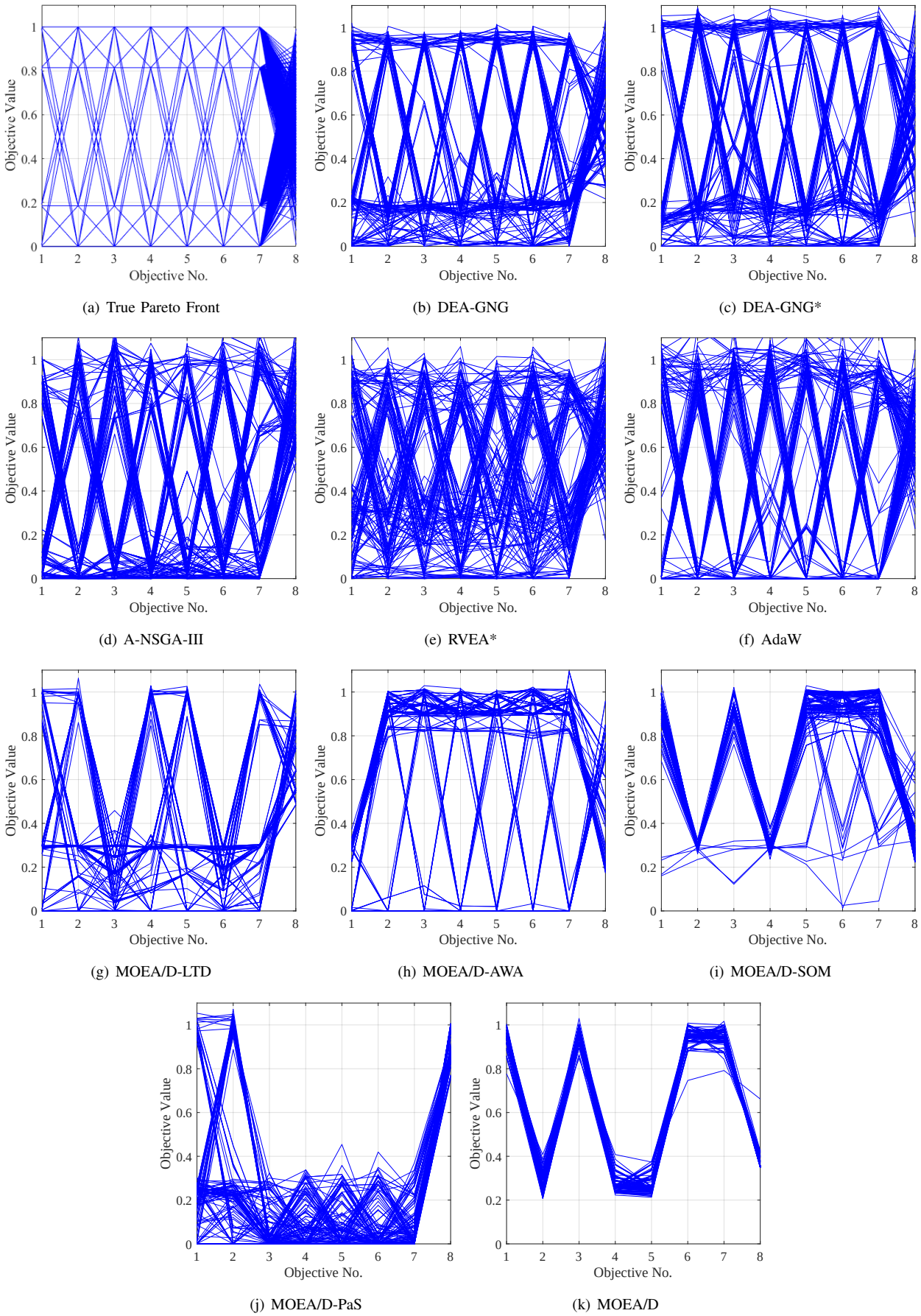

(a) True Pareto Front (b) DEA-GNG (c) DEA-GNG*

(d) A-NSGA-III (e) RVEA* (f) AdaW

(g) MOEA/D-LTD (h) MOEA/D-AWA (i) MOEA/D-SOM

(j) MOEA/D-PaS (k) MOEA/D

Fig. 2. The true Pareto front and the the final solution sets obtained by different algorithm in a single run on DTLZ7-8.

TABLE II
FRIEDMAN RANK TEST FOR THE RESULTS OF IGD$^+$

	Algorithms	Ranking
1	DEA-GNG	8.5882
2	AdaW	7.7353
3	DEA-GNG*	6.6471
4	MOEA/D-AWA	5.5294
5	RVEA*	5.5147
6	MOEA/D-LTD	5.4706
7	A-NSGA-III	5.4118
8	MOEA/D	4.0882
9	MOEA/D-SOM	3.4118
10	MOEA/D-PaS	2.6029
	p -value	9.039E-11

TABLE III
FRIEDMAN RANK TEST FOR THE RESULTS OF HV

	Algorithms	Ranking
1	DEA-GNG	7.5294
2	AdaW	6.8824
3	MOEA/D-AWA	6.4706
4	DEA-GNG*	6.2647
5	RVEA*	6.1765
6	A-NSGA-III	6.0294
7	MOEA/D-LTD	5.3824
8	MOEA/D-PaS	3.7353
9	MOEA/D	3.5588
10	MOEA/D-SOM	2.9706
	p -value	6.184E-11

the same as that of environmental selection, i.e., $O(N^2)$. When the input signal archive size and the population size are in the same order of magnitude, the time complexity of GNG update is $O(N^2)$ according to [15]. The time complexities of reference vector and scalarizing function adaptations are $O(N^2)$ and $O(N)$, respectively. Therefore, the total time complexity of the GNG-based learning model is also $O(N^2)$. To sum up, the total time complexity of DEA-GNG in one generation is $O(N^2)$. This implies that although the GNG-based learning model brings additional computation costs, the total time complexity of DEA-GNG is the same to those of most other MOEAs, such as NSGA-III [14].

III. FURTHER INVESTIGATIONS ON THE BEHAVIOR OF DEA-GNG

In this section, we investigate three important parameters, N_S, ϵ, and α to observe their effects on the behavior of DEA-GNG and thus to provide guidelines for setting them. In addition, we visualize the obtained GNG networks and the solution sets on the test problems with 3 objectives for a intuitive understanding.

A. Sensitivity Analysis of N_S

We applied DEA-GNG to Scalded DTLZ2 with 3 and 8 objectives with different settings of $|N_S|$. The results are shown in Fig. 3. We chose Scaled DTLZ2 since it has a relatively simple PF among the test problems, and it would be easy to observe the difference when changing N_S.

We can see from Fig. 3 that the average IGD$^+$ value slightly decreases while the runtime increases as N_S increases. This observation suggests that a larger value of N_S will improve the performance of DEA-GNG while consuming much more computation costs. However, the differences in the IGD$^+$ values are small. This means that DEA-GNG shows a robust performance under different settings of N_S. In this study, we set N_S to MN in the comparison with state of the art, where DEA-GNG obtained satisfying results with acceptable

TABLE IV
PAIRWISE HYPOTHESES ANALYZED BY THE POST-HOC TEST FOR THE RESULTS OF IGD$^+$

	Hypothesis	p -value
1	DEA-GNG vs. MOEA/D-PaS	3.6130E-16
2	DEA-GNG vs. MOEA/D-SOM	1.7968E-12
3	AdaW vs. MOEA/D-PaS	2.7621E-12
4	DEA-GNG vs. MOEA/D	8.8892E-10
5	AdaW vs. MOEA/D-SOM	3.9124E-09
6	DEA-GNG* vs. MOEA/D-PaS	3.6428E-08
7	AdaW vs. MOEA/D	6.8128E-07
8	DEA-GNG* vs. MOEA/D-SOM	1.0536E-05
9	DEA-GNG vs. A-NSGA-III	1.5200E-05
10	DEA-GNG vs. MOEA/D-LTD	2.1795E-05
11	DEA-GNG vs. RVEA*	2.8443E-05
12	DEA-GNG vs. MOEA/D-AWA	3.1059E-05
13	MOEA/D-AWA vs. MOEA/D-PaS	6.7390E-05
14	RVEA* vs. MOEA/D-PaS	7.3307E-05
15	MOEA/D-LTD vs. MOEA/D-PaS	9.4143E-05
16	A-NSGA-III vs. MOEA/D-PaS	1.3072E-04
17	DEA-GNG* vs. MOEA/D	4.9278E-04
18	A-NSGA-III vs. AdaW	1.5550E-03
19	AdaW vs. MOEA/D-LTD	2.0416E-03
20	RVEA* vs. AdaW	2.4943E-03
21	AdaW vs. MOEA/D-AWA	2.6645E-03
22	MOEA/D-AWA vs. MOEA/D-SOM	3.9285E-03
23	RVEA* vs. MOEA/D-SOM	4.1856E-03
24	MOEA/D-LTD vs. MOEA/D-SOM	5.0513E-03
25	A-NSGA-III vs. MOEA/D-SOM	6.4568E-03
26	DEA-GNG vs. DEA-GNG*	8.2047E-03
27	MOEA/D-PaS vs. MOEA/D	4.3104E-02
28	MOEA/D-AWA vs. MOEA/D	4.9691E-02
29	RVEA* vs. MOEA/D	5.2065E-02
30	MOEA/D-LTD vs. MOEA/D	5.9767E-02
31	A-NSGA-III vs. MOEA/D	7.1482E-02
32	DEA-GNG* vs. A-NSGA-III	9.2521E-02
33	DEA-GNG* vs. MOEA/D-LTD	1.0913E-01
34	DEA-GNG* vs. RVEA*	1.2306E-01
35	DEA-GNG* vs. MOEA/D-AWA	1.2800E-01
36	DEA-GNG* vs. AdaW	1.3835E-01
37	DEA-GNG vs. AdaW	2.4542E-01
38	MOEA/D-SOM vs. MOEA/D-PaS	2.7069E-01
39	MOEA/D-SOM vs. MOEA/D	3.5693E-01
40	A-NSGA-III vs. MOEA/D-AWA	8.7271E-01
41	A-NSGA-III vs. RVEA*	8.8851E-01
42	A-NSGA-III vs. MOEA/D-LTD	9.3615E-01
43	MOEA/D-LTD vs. MOEA/D-AWA	9.3615E-01
44	RVEA* vs. MOEA/D-LTD	9.5209E-01
45	RVEA* vs. MOEA/D-AWA	9.8402E-01

TABLE V
PAIRWISE HYPOTHESES ANALYZED BY THE POST-HOC TEST FOR THE RESULTS OF HV

	Hypothesis	p-value
1	DEA-GNG vs. MOEA/D-SOM	5.3567E-10
2	DEA-GNG vs. MOEA/D	6.4012E-08
3	AdaW vs. MOEA/D-SOM	9.9789E-08
4	DEA-GNG vs. MOEA/D-PaS	2.3802E-07
5	MOEA/D-AWA vs. MOEA/D-SOM	1.8758E-06
6	AdaW vs. MOEA/D	6.0100E-06
7	DEA-GNG* vs. MOEA/D-SOM	7.2578E-06
8	RVEA* vs. MOEA/D-SOM	1.2664E-05
9	AdaW vs. MOEA/D-PaS	1.8215E-05
10	A-NSGA-III vs. MOEA/D-SOM	3.1059E-05
11	MOEA/D-AWA vs. MOEA/D	7.3307E-05
12	MOEA/D-AWA vs. MOEA/D-PaS	1.9534E-04
13	DEA-GNG* vs. MOEA/D	2.2878E-04
14	RVEA* vs. MOEA/D	3.6419E-04
15	DEA-GNG* vs. MOEA/D-PaS	5.7191E-04
16	A-NSGA-III vs. MOEA/D	7.6686E-04
17	RVEA* vs. MOEA/D-PaS	8.8598E-04
18	MOEA/D-LTD vs. MOEA/D-SOM	1.0221E-03
19	A-NSGA-III vs. MOEA/D-PaS	1.7831E-03
20	DEA-GNG vs. MOEA/D-LTD	3.4567E-03
21	MOEA/D-LTD vs. MOEA/D	1.3017E-02
22	MOEA/D-LTD vs. MOEA/D-PaS	2.4897E-02
23	DEA-GNG vs. A-NSGA-III	4.1080E-02
24	AdaW vs. MOEA/D-LTD	4.1080E-02
25	DEA-GNG vs. RVEA*	6.5408E-02
26	DEA-GNG vs. DEA-GNG*	8.5016E-02
27	MOEA/D-LTD vs. MOEA/D-AWA	1.3835E-01
28	DEA-GNG vs. MOEA/D-AWA	1.4932E-01
29	DEA-GNG* vs. MOEA/D-LTD	2.2952E-01
30	A-NSGA-III vs. AdaW	2.4542E-01
31	RVEA* vs. MOEA/D-LTD	2.7950E-01
32	MOEA/D-SOM vs. MOEA/D-PaS	2.9769E-01
33	RVEA* vs. AdaW	3.3641E-01
34	DEA-GNG vs. AdaW	3.7822E-01
35	A-NSGA-III vs. MOEA/D-LTD	3.7822E-01
36	DEA-GNG* vs. AdaW	4.0028E-01
37	MOEA/D-SOM vs. MOEA/D	4.2309E-01
38	A-NSGA-III vs. MOEA/D-AWA	5.4797E-01
39	AdaW vs. MOEA/D-AWA	5.7497E-01
40	RVEA* vs. MOEA/D-AWA	6.8876E-01
41	DEA-GNG* vs. A-NSGA-III	7.4864E-01
42	DEA-GNG* vs. MOEA/D-AWA	7.7919E-01
43	MOEA/D-PaS vs. MOEA/D	8.1008E-01
44	A-NSGA-III vs. RVEA*	8.4127E-01
45	DEA-GNG* vs. RVEA*	9.0436E-01

TABLE VI
TIME COMPLEXITY OF DEA-GNG IN ONE GENERATION

	Operator	Complexity
DEA-Based Optimization Model	Mating Selection	$O(N)$
	Offspring Reproduction	$O(N)$
	Environmental Selection	$O(N^2)$
	Total of DEA	$O(N^2)$
GNG-Based Learning Model	Input Signal Archive Update	$O(N^2)$
	GNG Update	$O(N^2)$
	Reference Vector Adaptation	$O(N^2)$
	Scalarizing Function Adaptation	$O(N)$
	Total of GNG	$O(N^2)$
	Total of DEA-GNG	$O(N^2)$

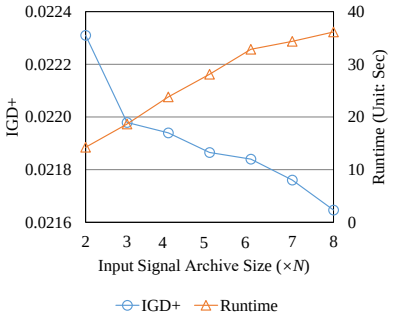

(a) 3-objective Scaled DTLZ2

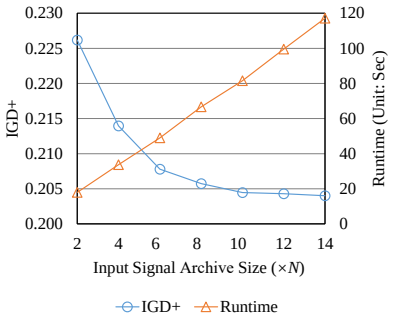

(b) 8-objective Scaled DTLZ2

Fig. 3. The results on Scaled DTLZ2 under different settings of N_S.

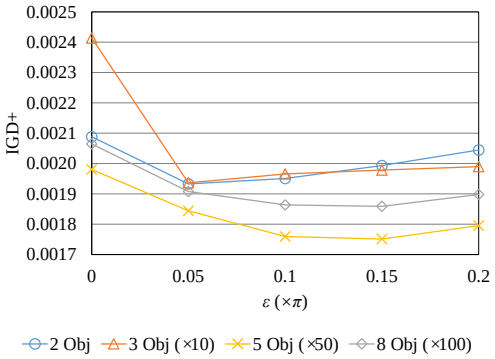

Fig. 4. The results on DTLZ7 under different settings of ϵ.

computation costs.

B. Sensitivity Analysis of ϵ

We used DTLZ7 with 2, 3, 5, and 8 objectives to investigate the effect of ϵ. DTLZ7 has a relatively complex PF. The best θ value for each reference vector could be different. Fig. 4 shows the results on DTLZ7 under different settings of ϵ, where 3 Obj ($\times 10$) represents the IGD$^+$ results on 3-objective DTLZ7 which should be multiplied by 10. 2 Obj, 5 Obj ($\times 50$), and 8 Obj ($\times 100$) have similar meanings.

From Fig. 4, we can see that subtracting ϵ leads to a better IGD$^+$ results than not in all cases. The good IGD$^+$ results were obtained in a wide range of values of ϵ (i.e., $[0.05, 0.2]$) for DTLZ7 with 2, 3, 5, and 8 objectives. This observation shows the robust performance of DEA-GNG. Furthermore, $\epsilon =$

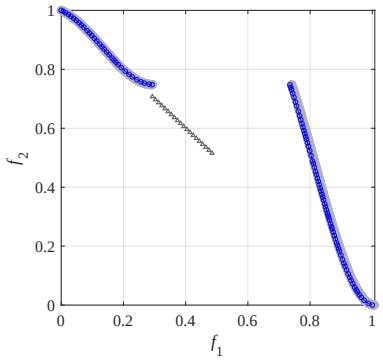

(a) The final reference vectors in the normalized objective space

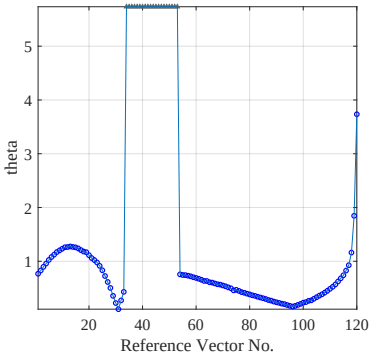

(b) θ corresponding to the reference vectors

Fig. 5. The final reference vectors and the corresponding θ values when ϵ is set to 0.05π in a typical run on 2-objective DTLZ7. The triangles and the circles represents the reference vectors from R'_u (i.e., uniformly generated reference vectors) and R'_{node} (i.e., nodes in the GNG network), respectively. In (a), the shaded region is the true PF. In (b), the reference vectors are sorted in ascending order according to their first objective values (i.e., f_1), and the triangles on the top mean that θ is ∞.

0.05π is a slightly better setting for DTLZ7 with 2 and 3 objectives, while $\epsilon = 0.15\pi$ is a slightly better setting for DTLZ7 with 5 and 8 objectives. This implies that we can increase the value of ϵ to improve the algorithm's performance when solving MaOPs.

In addition, in Fig. 5 we present the final reference vectors and the corresponding θ values when ϵ is set to 0.05π in a typical run on 2-objective DTLZ7 for an intuitive understanding of the proposed scalarizing function adaptation. In Fig. 5 (a), the triangles and the circles represents the reference vectors from R'_u (i.e., uniformly generated reference vectors) and R'_{node} (i.e., nodes in the GNG network), respectively. The shaded region is the true PF. In Fig. 5 (b), the reference vectors are sorted in ascending order according to their first objective values (i.e., f_1), and the triangles on the top mean that θ is ∞. We can observe from Fig. 5 that the proposed scalarizing function adaptation can adjust θ according to the PF shape.

C. Sensitivity Analysis of α

We used DTLZ7 with 3 objectives to investigate the effect of α. Similar results were also obtained on other test problems, which are not provided here. Fig. 6 shows the results of DEA-GNG on DTLZ7 under different settings of α.

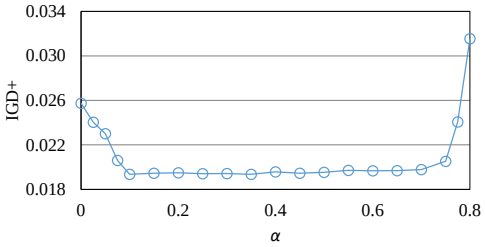

Fig. 6. The results on DTLZ7 under different settings of α.

From Fig. 6 we can see that the algorithm achieves good performance when α is in the range of [0.1, 0.7]. Either a too large value (larger than 0.7) or a too small value (smaller than 0.1) of α clearly deteriorates the performance. This implies that (1) when the algorithm approaches the end of the search process, no change to the reference vectors and the scalarizing functions can improve the performance by making the algorithm to focus on exploitation; (2) stopping the GNG-based learning model too early results in inappropriate reference vectors and scalarizing functions. Since we usually cannot know when the GNG network can well represent the true PF shape during the search process, we set α to be a relatively small value (i.e., 0.1) in this study. It is worth noting that AdaW [4] also does not change the weight vectors during the last 10% generations for the same reason.

D. Visualization of the obtained GNG networks

Fig. 7 shows the obtained GNG networks at the end of evolution on all the test problems with 3 objectives in a single run to visually investigate the performance of DEA-GNG. In each sub-figure, the circles and lines are the nodes and the edges in the GNG network, respectively, and the shaded region is the true PF. We can see from Fig. 7 that the GNG networks are very close to the true PF shapes.

REFERENCES

[1] J. Bader and E. Zitzler, "HypE: An algorithm for fast hypervolume-based many-objective optimization," *Evolutionary Computation*, vol. 19, no. 1, pp. 45–76, 2011.

[2] H. Jain and K. Deb, "An evolutionary many-objective optimization algorithm using reference-point based nondominated sorting approach, part II: Handling constraints and extending to an adaptive approach." *IEEE Trans. Evolutionary Computation*, vol. 18, no. 4, pp. 602–622, 2014.

[3] R. Cheng, Y. Jin, M. Olhofer, and B. Sendhoff, "A reference vector guided evolutionary algorithm for many-objective optimization," *IEEE Transactions on Evolutionary Computation*, vol. 20, no. 5, pp. 773–791, 2016.

[4] M. Li and X. Yao, "What weights work for you? adapting weights for any pareto front shape in decomposition-based evolutionary multi-objective optimisation," *arXiv preprint arXiv:1709.02679*, 2017.

[5] M. Wu, K. Li, S. Kwong, Q. Zhang, and J. Zhang, "Learning to decompose: a paradigm for decomposition-based multiobjective optimization," *IEEE Transactions on Evolutionary Computation*, vol. 23, no. 3, pp. 376–390, 2018.

[6] Y. Qi, X. Ma, F. Liu, L. Jiao, J. Sun, and J. Wu, "MOEA/D with adaptive weight adjustment," *Evolutionary Computation*, vol. 22, no. 2, pp. 231–264, 2014.

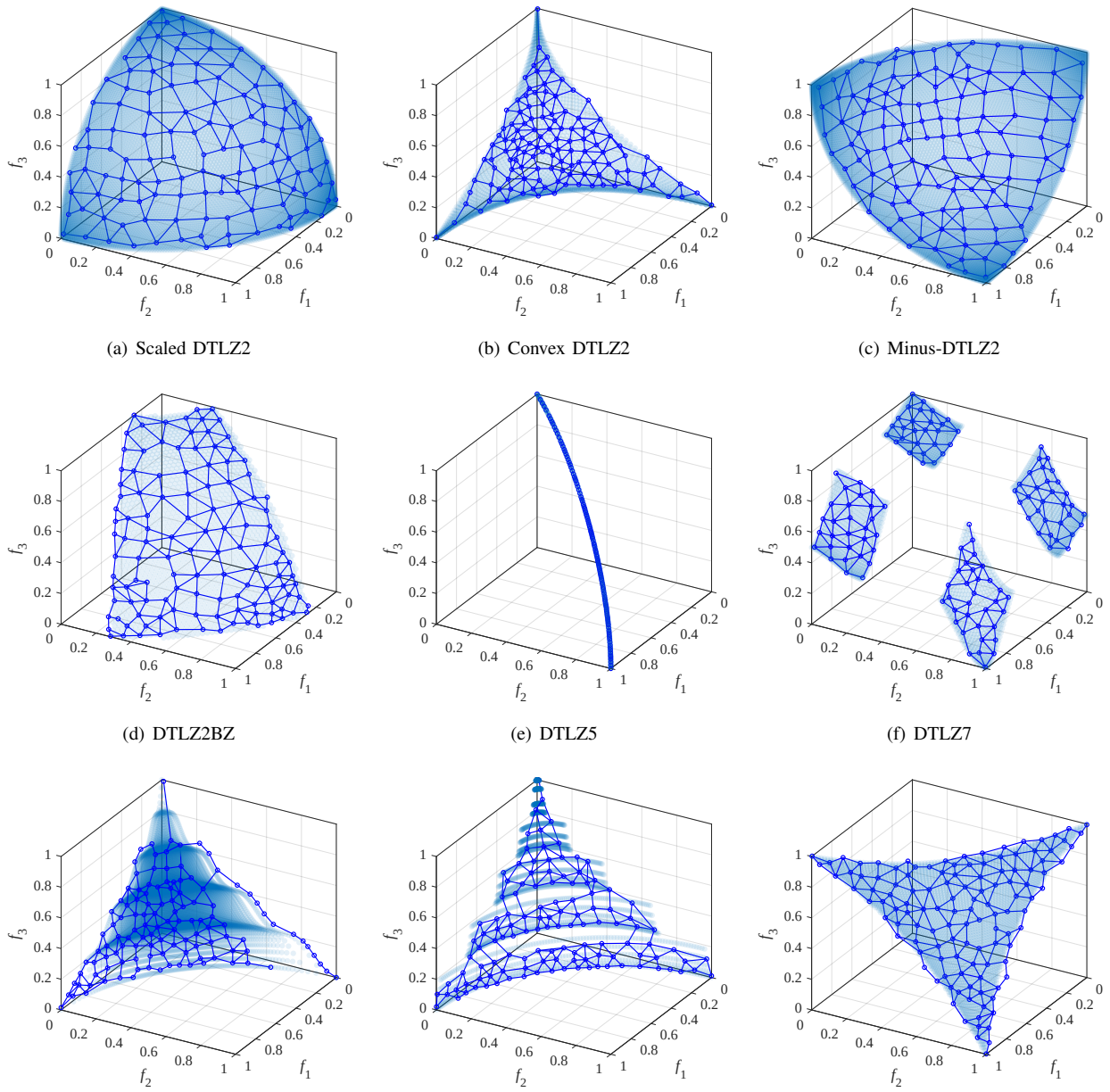

(a) Scaled DTLZ2 (b) Convex DTLZ2 (c) Minus-DTLZ2

(d) DTLZ2BZ (e) DTLZ5 (f) DTLZ7

(g) WFG1 (h) WFG2 (i) Polygon-Based Problem

Fig. 7. The obtained GNG networks in a single run. In each sub-figure, the circles and lines are the nodes and the edges in the GNG network, respectively, and the shaded region is the true PF.

[7] F. Gu and Y.-M. Cheung, "Self-organizing map-based weight design for decomposition-based many-objective evolutionary algorithm," *IEEE Transactions on Evolutionary Computation*, vol. 22, no. 2, pp. 211–225, 2018.

[8] R. Wang, Q. Zhang, and T. Zhang, "Decomposition-based algorithms using pareto adaptive scalarizing methods," *IEEE Transactions on Evolutionary Computation*, vol. 20, no. 6, pp. 821–837, 2016.

[9] Q. Zhang and H. Li, "MOEA/D: A multiobjective evolutionary algorithm based on decomposition," *IEEE Transactions on Evolutionary Computation*, vol. 11, no. 6, pp. 712–731, 2007.

[10] H. Ishibuchi, R. Imada, N. Masuyama, and Y. Nojima, "Comparison of hypervolume, IGD and IGD+ from the viewpoint of optimal distributions of solutions," in *International Conference on Evolutionary Multi-Criterion Optimization*. Springer, 2019, pp. 332–345.

[11] M. Li and X. Yao, "Quality evaluation of solution sets in multiobjective optimisation: A survey," *ACM Computing Surveys (CSUR)*, vol. 52, no. 2, p. 26, 2019.

[12] M. Li, L. Zhen, and X. Yao, "How to read many-objective solution sets in parallel coordinates [educational forum]," *IEEE Computational Intelligence Magazine*, vol. 12, no. 4, pp. 88–100, 2017.

[13] J. D. Gibbons and S. Chakraborti, *Nonparametric statistical inference*. Springer, 2011.

[14] K. Deb and H. Jain, "An evolutionary many-objective optimization algorithm using reference-point based non-dominated sorting approach, part I: Solving problems with box constraints," *IEEE Transactions on Evolutionary Computation*, vol. 18, no. 4, pp. 577–601, 2013.

[15] Y. Quintana-Pacheco, D. Ruiz-Fernández, and A. Magrans-Rico, "Growing neural gas approach for obtaining homogeneous maps by restricting the insertion of new nodes," *Neural Networks*, vol. 54, pp. 95–102, 2014.